

Connecting and disconnecting for chain self-reconfiguration with PolyBot

Mark Yim Ying Zhang Kimon Roufas David Duff
 Craig Eldershaw
 Palo Alto Research Center, CA, USA.

Abstract—

Chain modular robots form systems with many degrees of freedom which are capable of being reconfigured to form arbitrary chain-based topologies. This reconfiguration requires the detaching of modules from one point in the system and re-attaching at another. The internal errors in the system (especially with large numbers of modules) are such that accurate movement of chain ends, required for the attaching of modules, can be extremely difficult. A three phase docking process is described that utilizes both open and closed-loop techniques.

This process has been shown to work with an early version. Issues raised during this testing have been addressed in a later version. Discussion of these issues, their solutions and preliminary results of the testing the latest version are given.

Index Terms—PolyBot, robot, chain, reconfigurable

I. INTRODUCTION

A. N -Modular reconfigurable robot systems

A Modular Reconfigurable Robot is constructed from a large number of discrete modules. Each module is capable of being mechanically (and usually electrically) connected to one or more other modules. Such a system is described as n -modular robot if there are n different module types. n is usually far less than the total number of modules in the system. While the capabilities of a single module, which may only have one active degree of freedom, are exceedingly modest, the combination can form an arbitrarily complex structure.

As the properties of a robot changes with it's form, then a robot that can change its form is extremely versatile. Figure 1 shows just a few forms that PolyBot, a particular modular self-reconfigurable robot, has achieved. A self-reconfigurable robot is one that is able to change from one form to another with no external mechanical assistance.

As well as enabling versatility, the massively redundant nature of the system can lead to robustness—and even self-repair. A third hope, is that economies of scale and batch fabrication of many identical modules may eventually lead to low cost. [1], [2].

It must be recognized that this versatility does come at a cost. Single task systems can, in general, be made cheaper, faster and more efficient than a system that can achieve multiple tasks. Modular reconfigurable systems are thus suited for those applications which *require* versatility, or when the task parameters are not known in advance.

Exploration tasks are good examples of where modular self-reconfigurable robots can excel. In planetary exploration, the

types of terrain may not be known. In search and rescue in a rubble pile and other unstructured environments, the types of locomotion that are needed may not be known. Thus a reconfigurable robot has the versatility to adapt to the changing requirements of unknown tasks where specialized robots may fail.

Some modular systems are manually reconfigurable, [3], [4] and others are self-reconfigurable [5], [6], [7], [8], [9], [10], [11], [12], [13], [14], [15], [16], [17], [18], [19], [20], [21]. Some properties that all of these systems share is the ability to connect and disconnect from modules with a set of mating connectors. Self-reconfiguration is the automatic process of rearranging the modules. It requires the planning of several aspects: the sequence of connectivity changes; the collision-free motion of the modules; and the control of docking, latching and unlatching of the modules.

B. Self-reconfiguration classification

We can classify most self-reconfiguring systems into three classes based on the method of reconfiguration: mobile reconfiguration, lattice reconfiguration and chain reconfiguration. [5]

1) *Mobile*: Mobile reconfiguration systems use the environment to maneuver modules to dock with other modules. Examples include Fukuda's early CEBOT [6], Hirose's UniRover [7] and Brown's millibot trains [8].

2) *Lattice*: Lattice reconfiguration systems change shape by moving into positions on a virtual grid, or lattice. Modules may move only to neighboring positions within the lattice. Planning and control is well structured for local control since the robot need only deal with what is occupying the small number of neighboring positions in the lattice. Prototype systems that use lattice reconfiguration include [2], [9], [10], [11], [12], [13], [14], [15].

3) *Chain*: The chain reconfiguration systems reconfigure themselves by attaching and detaching chains of modules to and from themselves, with each module connected to every other at least indirectly. That is, the system remains as one connected component.

Systems that use chain reconfiguration include [16], [17]. Figure 1 shows PolyBot (a chain robot) at three stages of self-reconfiguration where it transforms from a loop to a snake to a figure-8 then to a four legged configuration. Forming the figure-8 was aided by some teleoperation.

Shen *et al* have explored docking with CONRO, a chain reconfiguration system described in [17], using a light based search for chain motions in a plane. This paper also focuses on

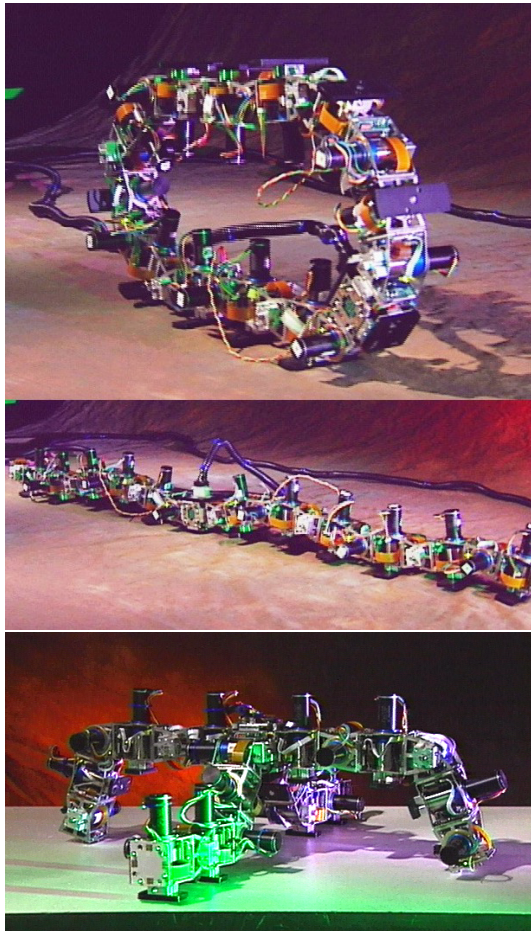


Fig. 1. PolyBot G2 modules in three configurations

chain reconfiguration systems, with specific reference to PolyBot. In the proposed approach, the process is divided into three phases; two of these are closed loop in nature, which is more efficient than a search.

While this paper focuses on chain reconfiguration, many of the properties of docking and releasing apply to the mobile class and lattice class of reconfiguration as well.

Following this introduction is a description of chain reconfiguration, in particular describing the connection and disconnection process. Sections III and IV describe the connection process for two generations of PolyBot.

II. CHAIN RECONFIGURATION MAKING/BREAKING LOOPS

As chain reconfiguration occurs, the joining and splitting of loops requires modules to attach and detach from other modules. Detaching is empirically easier than latching since the chain is essentially breaking and primarily simply requires the proper mechanical design with little closed-loop control.

A. Automatic disconnect

There are a variety of methods to disconnect chains of modules in modular robots. This may happen by the turning of a screw, releasing hooks [10], [18], [19], (dis)engaging electromagnets [2], [13], turning off permanent switching magnets

[11], as well as others. In some systems, where docking and subsequent re-latching is not required, single-use mechanisms such as explosive bolts have been employed.

PolyBot Generation 1 (aka “G1”, an early version of PolyBot) used such a singly-use method of unlatching. This was used to demonstrate reconfiguring into two topologically different styles of locomotion [1]. A loop configuration initially rolled like a tread, then opened up to a snake-like configuration and uses a undulating gait.

The system was a serial chain where one end had a slotted hole, and the other end a T-shaped bar, whose top part mates with the slot. These two ends are initially inserted manually and twisted to lock them together (closing the chain into a loop). The device had no direct mechanism for latching or unlatching, instead it requires the twisting motion of the rest of the chain to align the bar with the slot. If a tension bias is applied while the two ends are appropriately aligned, then the chain simply falls apart. Re-docking was theoretically possible by using inverse kinematics to move the joints so as to re-insert the bar through the slotted hole. However imprecision in the joints made this infeasible in practice. Either the mechanism must be made more tolerant to mis-alignment, or else the position control must be made more precise.

B. Docking and latching

The forming of loops has two distinct phases,

- 1) an approach (or docking) of two connectors, and
- 2) the latching of the connector mechanism.

This part of the reconfiguration is significantly more complicated than the disconnection of modules, as both careful coordination and accurate control are required.

The precision required for the docking phase is highly dependent on the actual latching mechanism. Typically the mechanism is designed to minimize the level of precision required, permitting at least some error in all six degrees of relative freedom between the two mating faces. Nilsson has studied the geometry and other issues relevant to minimize the level of precision required for docking.[20]

In closed chain reconfiguration, the approach also involves planning the collision free motion of the chains prior to the actual docking. For chains with many modules and many degrees of freedom, the inverse kinematics and collision free planning is difficult. This is especially the case for highly complex systems, where self-collision may involve the coordinated motion of chains other than those directly involved in the mating.

The rest of this paper addresses only the automatic docking and attaching process. For information on collision free motion and the connectivity planning problem, the reader is referred to [21] and [5].

III. POLYBOT G2 CONNECTION

PolyBot is a chain reconfiguration system that will be used to highlight methods and issues in the docking requirements of self-reconfiguration.

Like PolyBot G1, Generation 2 is also a 2-modular reconfigurable robot system. That is, it is constructed from two module types: nodes and segments. The segment modules are nom-

inally rectangular prisms and have one rotational degree of freedom separating two connection ports. The node modules are fixed cubes (i.e. entirely passive) with six connection ports.

Unlike its G1 predecessor, G2's connection ports have electromechanical latches under software control. These latch onto the pins protruding from the opposite face. An IR ranging system permits closed loop docking as will be elaborated on in this section. A G2 segment module can be seen in Figure 2.

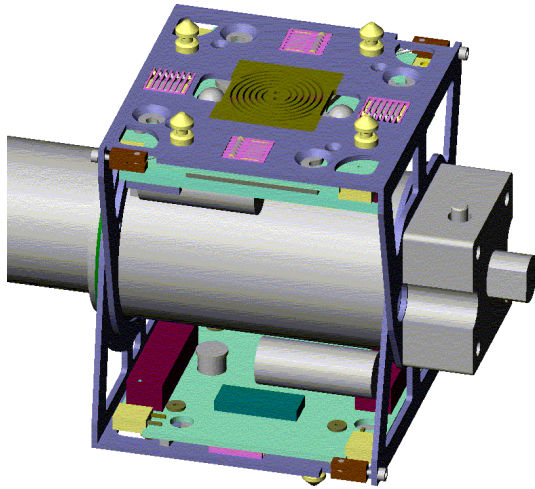


Fig. 2. CAD rendering of a PolyBot G2 module

G2 segments are roughly $L \times W \times H = 60 \times 70 \times 110$ mm (where the length, L , is the distance between the two opposing interface plates when held parallel). The main internal components of a G2 segment are: the brushless DC motor with gear box, interface plates, motor drive circuit board, and a CPU board. Each module has a Motorola PowerPC 555 embedded processor with: 448kb of internal reprogrammable program store (FLASH memory), 1Mb of external data SRAM, and the ability to communicate using Controller Area Network (or CAN, a robust shared bus communications protocol). Besides the IR ranging components, the only other sensors are the hall-effect sensors built into the brushless DC motors. These are used to commutate the brushless motor and to keep track of the angular orientation of the two sides of each segment module.

As can be seen in the rendering of the G2 Segment (Figure 2), the interface plates (approximately 50×50 mm) are quite crowded. Some visible aspects include: the electrical interface elements, which are hermaphroditic; the grooved pins and holes that repeat at 90° intervals about the center; the latch return spring; and the IR sensors and emitters.

The 90° repetition of pins, holes and electrical connectors allows the modules to mate in any of four orientations. The hermaphroditic property of the plates allows every interface plate to be the same and so any plate can mate with any other interface plate. This is in contrast with some other reconfigurable robots where docking is more restricted due to having the male types and female types.

When two modules are attached together the grooved pins on one plate penetrate through the holes in the other plate. A hook-like latch is engaged in the groove on the pin to lock the modules rigidly together.

The latch mechanism is quite simple in concept however the many dependencies between parts and the 2mm thick available volume complicate the implementation. The latch plate (laser cut from SS 304 sheet) rotates about the center of the interface as seen in Figure 3. Its four legs reach out and around the grooves in the pins of a mating module when the latch is engaged. Two pieces of 150 micron shape memory alloy (SMA) wire are mechanically connected to (but electrically isolated from) the plate. These wires extend out, around a pin in a turnbuckle on the corners of the plate and return to the latch plate. Electrical connections are made to the two ends of the SMA wire where they are attached to the latch plate.

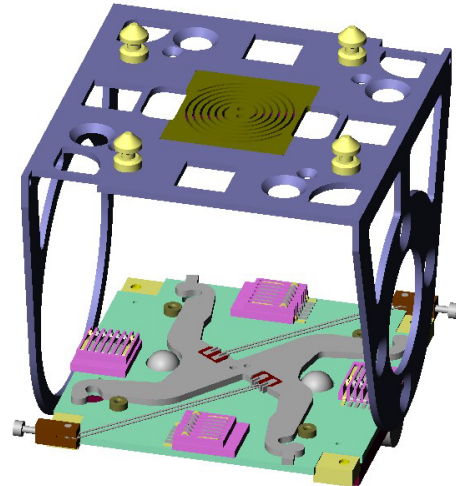


Fig. 3. Rendering of back side of connection plate of PolyBot G2

When current is passed through the SMA wires, coulomb heating occurs and the wires contract ($\approx 4\%$) causing the latch plate to rotate. When the current is shut off the wires cool below their transition temperature and a return spring returns the latch to the engaged position. Note that the latch is thus passive when engaged (requiring no energy) and active only during a release transition. The return spring is made from 1mm thick BeCu sheet metal and is press-fit into the frame. The spring is a pair of 2.5 turn spirals wire-EDM cut into BeCu sheet. The latch plate is pinned to the spring during assembly.

Disconnecting two modules is straight-forward, the two modules simply open their SMA-driven latches, and then move away from each other. Connecting two modules is theoretically the same, however the positional accuracy required for the pins to enter is considerable.

With large chains of PolyBot modules, the positional error from end to end increases. This error is due to both inaccuracies in angle measurement (i.e. the module hasn't bent to quite the angle it thinks it is) and mechanical slop at the interface plates.

This problem was anticipated, and the mechanical design aims to reduce the required accuracy. The chamfers on the pins and holes guide the pins into the latch hole as the plates come together. The chamfered holes have an outer diameter of 6mm at the face, the pins come nearly to a point, removing up to 3mm of translational error or 8° of rotational error.

However even these tolerances can be exceeded over a long chain of modules, and so the remainder of this section discusses

the control strategies employed.

The overall process has three distinct phases, in this way it is similar to the work on CONRO described in [22]. The first is the long range phase; this brings two modules in proximity to each other from arbitrarily far distances using just joint angle sensors. Once close enough that the IR sensors on the two docking modules can sense the opposing module, then the medium range phase begins. This brings the modules closer together, close enough so that the short range process can finish the docking. It is at this stage that the mechanical properties discussed above come into play. Using only joint angle information, the short range process applies forces in different directions to push the modules together until latched.

For the PolyBot G2 modules, the medium phase is designed to be effective with independent starting errors of up to: 30mm of translational error; $\approx 20^\circ$ rotational error in roll; and $\approx 40^\circ$ of rotational error in each of yaw and pitch. So the long range process must terminate with the two modules being within these bounds.

The short range process can tolerate up to 3mm of translational error and 8° of rotational error. So the medium range process must achieve at least this level before concluding.

A. Long range

Inverse kinematics is used in all of the docking phases, though the exact manner in which it is employed does vary. In the long range phase, one of the mating modules calls the inverse kinematics routine with a fixed goal position, aiming for the middle of the region which is feasible for starting the medium range phase. The inverse kinematics routine calculates the joint angles for each segment module to achieve the goal position.

For self-reconfiguring systems that can adopt arbitrary configurations, no assumptions can be made about the configuration immediately prior to any reconfiguration. And so the kinematic model of the system (and in particular the chains being joined) must be generated on the fly. Denavit-Hartenberg (DH) notation is used for the representation of a chain of modules. Assume the size of the module is an $L \times L \times L$ cube. Given two connected PolyBot segments, the DH Parameters (a, α, d) are as follows: a is L , the distance between the two axes of rotation; α is $0^\circ, 90^\circ, 180^\circ$ or 270° , depending on the connection; and d is always 0. In the case where there are nodes (the passive modules) between the segments, then $a = (n + 1)L$, where n is the number of nodes.

Given a reference frame associated with a module in a chain, let θ_i be the joint angle of the module that is i th positions from the reference module. Then $DH[i]$ is the DH Parameters of that module and a transformation matrix $T_i(\theta_i)$ can be generated. Let the docking module be the n th in the chain. The transformation of the docking module with respect to the reference frame is

$$T(\theta_1, \dots, \theta_n) = \prod_{i=1}^n T_i(\theta_i) \cdot T_e$$

where T_e is the transformation moving $L/2$ in x -direction. Using T , the 6D offset of the docking face from the reference frame may be obtained.

For the long range docking process, either a fixed goal position, or else the transformation T_g of the docking face is given. T_g is the approximate position of the other docking face with respect to the reference frame. The inverse kinematics routine is to calculate the θ_i from equation $T(\theta_1, \dots, \theta_n) = T_g$.

This reduces to six equations with n variables. A generalised constraint solver is implemented using Newton's Method with a singular value decomposition (SVD) at each Newton's step. SVD is robust for both under- and over-constrained problems (i.e. for any n). In order to improve the solution quality, the Jacobian matrix is calculated analytically instead of estimating it numerically. For each transformation $T_i(\theta_i)$,

$$T'(\theta_i) = \left[\prod_{j=1}^{i-1} T_j(\theta_j) \right] \cdot T'_i(\theta_i) \cdot \left[\prod_{j=i+1}^n T_j(\theta_j) \right].$$

B. Medium range

A major part of the docking process is the closed-loop control in the medium range phase. Here the relative position of the two docking plates are directly sensed in six dimensions using infrared (IR) emitters and detectors. Figure 4 shows the mechanical design of the plate, with IR emitters at each of the four corners, and two IR receivers (phototransistors) in the center.

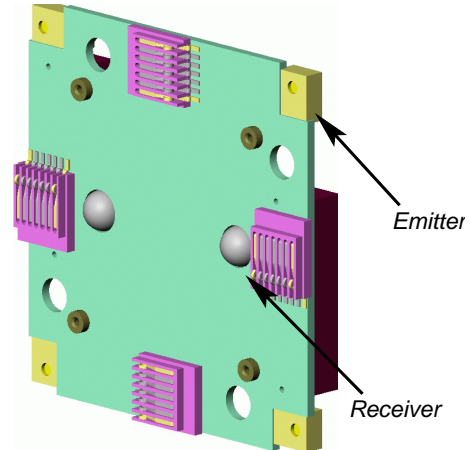


Fig. 4. Mechanical design of the IR 6D sensing device on a PolyBot faceplate.

The IR system is used to determine the direction of motion required to close the distance between the two plates. Two separate methods for calculating this distance are discussed below.

Once the 6D relative offset is found, by whichever method, inverse kinematics provides the joint angle movements which will effect this change. The same inverse kinematics routines used in the long range process (described above) are employed again, except that T_g is not given as fixed, but rather computed from $T \cdot T_o$. T is the current transformation matrix and T_o is the desired offset between two docking faces, calculated from the IR measurements.

Small incremental steps are used for each motion, until the plates are within the range for the final phase.

1) *Computed offset method:* Each receiver senses the intensity of light received when individual opposing emitters are lit in sequence. The intensity of light measured at a receiver is a

function of both the distance between the emitter and receiver, and also their angular offset (i.e. the angle between the imaginary centerlines of the emitters and receivers). A model of the IR emitter/receivers can be created yielding equations which use these parameters. For any given sensor data, the equations can be solved to find the 6D offset between two plates. This is the information the inverse kinematics solver requires. The performance of this process is discussed in Section III-D.

Figure 5 shows the control signals for the lighting of the first four emitters. Each face is allocated one time slot (slot one or two). The two sides are synchronized periodically through the independent wired communications bus.

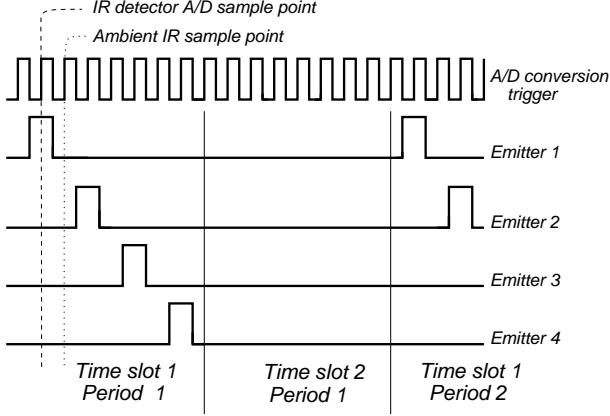


Fig. 5. Emitting and receiving sequence.

At the end of a time slot, each of the four receivers (two on each plate) will have eight readings: one from each of the opposite four emitters, and four measurements of the ambient light. Subtracting the ambient readings from the actual sample (to increase robustness to external IR noise) gives a total of sixteen pieces of data.

In each MPC555 processor on the two mating modules, a Time Processing Unit (TPU3) generates the trigger and emitter control signals. The trigger signal is fed back into the same chip to activate an on-chip queued analog to digital converter (A/D). The A/D values returned reflect the current IR intensity at each receiver. Being a queued system, then a single trigger pulse causes a sample at all four receivers followed by a single interrupt. The interrupt service routine is responsible for subtracting the previously taken ambient light readings and sending the results to the appropriate destination. This message travels over the independent wired communications bus. Whichever module is currently doing the overall coordination of motion will receive the sets of data from both faces and issue movement commands accordingly.

For each plate, consider attaching a frame as shown in Figure 6 (in this case Plate 1 and Plate 2 are facing each other). Given an offset between the two plates, the spatial relationship between every combination of emitter and receiver can be determined.

Let d be the distance from the receiver to the center of the plate, and w and h be the width and height of the position of the emitters. The coordinate of receiver 1, in its own frame, is $\langle 0, 0, d \rangle$, and the coordinate of receiver 2 is $\langle 0, 0, -d \rangle$; similarly, the coordinates of emitters A, B, C and D

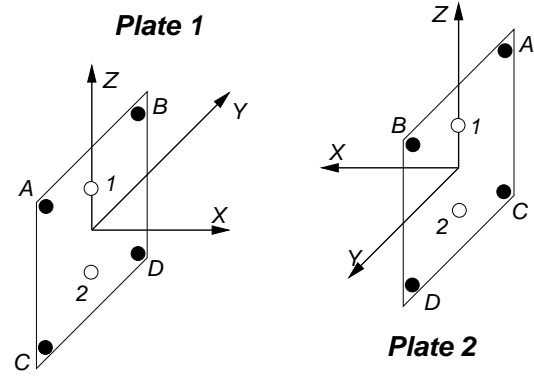


Fig. 6. Frames for plates.

are $\langle 0, -w, h \rangle$, $\langle 0, w, h \rangle$, $\langle 0, -w, -h \rangle$ and $\langle 0, w, -h \rangle$, respectively. Let $\langle x, y, z, \alpha, \beta, \gamma \rangle$ be the offset of the frame of plate 2 with respect to the frame of plate 1 (e.g. in the case of two plates exactly aligned facing each other, the offset is $\langle x, 0, 0, \pi, 0, 0 \rangle$). Let T be the transformation matrix from plate 1 to plate 2 obtained by the offset, and R be the rotation matrix of T . The norm of plate 1 is $\langle 1, 0, 0 \rangle$ and the norm of the plate 2, in plate 1 coordinates, is $R\langle 1, 0, 0 \rangle$. Let $\langle x_e, y_e, z_e \rangle$ be the coordinate of the emitter in its own frame and $\langle x_r, y_r, z_r \rangle$ be the coordinate of the receiver of the opposing plate in its own frame. There are two cases:

- The emitter is on plate 1 and the receiver is on plate 2: the position of the emitter is $\vec{\sigma} = \langle x_e, y_e, z_e \rangle$ and the position of the receiver is $\vec{q} = T\vec{p}$, where $\vec{p} = \langle x_r, y_r, z_r \rangle$ and $\vec{q} = \langle x'_r, y'_r, z'_r \rangle$.
- The emitter is on plate 2 and the receiver is on plate 1: the position of the receiver is $\vec{\sigma} = \langle x_r, y_r, z_r \rangle$, and the position of the emitter is $\vec{q} = T\vec{p}$, where $\vec{p} = \langle x_e, y_e, z_e \rangle$ and $\vec{q} = \langle x'_e, y'_e, z'_e \rangle$.

Given two points in space, $\vec{\sigma}$ and \vec{q} , and the norms of their plates, \vec{n}_o and \vec{n}_q , then: the distance between them is $|\vec{q} - \vec{\sigma}|$; the angle at $\vec{\sigma}$ is $\arccos(\vec{n}_o \cdot (\vec{q} - \vec{\sigma}) / |\vec{q} - \vec{\sigma}|)$; and the angle at \vec{q} is $\arccos(\vec{n}_q \cdot (\vec{\sigma} - \vec{q}) / |\vec{q} - \vec{\sigma}|)$. Therefore the emitter and receiver angles, as well as the distance between the receiver and the emitter, can be obtained for each of the sixteen pairs of emitters and receivers. An IR intensity model was obtained by measuring intensities over a set of angular and distance displacements, and then fitting the theoretical curve to those data points. The 6D offset can be calculated using this model and the sixteen measurements $I_i = f_i(x, y, z, \alpha, \beta, \gamma)$, for $i = 1, \dots, 16$.

Theoretically, the same constraint solver described above for use in finding inverse kinematics could be used to solve this over-constrained set of equations. However in practice, the IR model obtained was found to be numerically sensitive to sensor mounting errors, and was not accurate enough for robust estimation. This unfortunate shortcoming is elaborated on, in Section III-D. As an alternative, the centering method, described next, was adopted.

2) *Centering method:* The centering method is based upon the idea that the measured intensities should be balanced (equal) when the plates are centered and facing each other. The method is far more robust to sensor model errors and numerical ill-conditioning.

This method differs from the computed offset method outlined above, in that the result is not a single 6D offset which could (theoretically) be compensated for in one movement. Rather, it gives a quickly computed indication of the general direction of movement required. By making repeatedly measuring, calculating and moving, the two modules should progressively decrease their relative offset.

Let X_{ij} represent a reading where X is the emitter ID (A , B , C , or D), i is the receiver ID (1 or 2) and j is the plate ID (1 or 2), and let \star represent the case that holds for both plate 1 and 2. When two plates are centered and facing each other, we have a set of equations, e.g., $A_{1\star} = B_{1\star}$, $A_{2\star} = B_{2\star}$, $C_{1\star} = D_{1\star}$ and $C_{2\star} = D_{2\star}$. In practice, even when the two plates are exactly centered, the equations may not hold because of noise and slight variations when mechanically assembling the plates. The difference, however, can be used as a guideline for a relative offset. For example, $(A_{1\star} - B_{1\star}) + (A_{2\star} - B_{2\star}) + (C_{1\star} - D_{1\star}) + (C_{2\star} - D_{2\star})$ gives offset in the Y direction, while $(A_{1\star} - C_{2\star}) + (A_{2\star} - C_{1\star}) + (B_{1\star} - D_{2\star}) + (B_{2\star} - D_{1\star})$ gives relative offset in the Z direction.

Consideration of the geometry and some simple calculations yields five sets of equations. Each set is associated with one of the 6D offset dimensions, and is invariant under changes in that dimension.

- $B_{12} + D_{22} + B_{11} + D_{21} = A_{12} + C_{22} + A_{11} + C_{21}$ and $B_{22} + D_{12} + B_{21} + D_{11} = A_{22} + C_{12} + A_{21} + C_{11}$ hold true as Y changes.
- $A_{12} + B_{12} + D_{21} + C_{21} = C_{22} + D_{22} + B_{11} + A_{11}$ and $A_{22} + B_{22} + D_{11} + C_{11} = C_{12} + D_{12} + B_{21} + A_{21}$ hold true as Z changes.
- $B_{12} + A_{11} + D_{22} + C_{21} = A_{12} + B_{11} + C_{22} + D_{21}$ and $D_{12} + C_{11} + B_{22} + A_{21} = C_{12} + D_{11} + A_{22} + B_{21}$ hold true as α changes.
- $A_{12} + B_{11} + B_{12} + A_{11} = C_{22} + D_{21} + D_{22} + C_{21}$ and $A_{22} + B_{21} + B_{22} + A_{21} = C_{12} + D_{11} + D_{12} + C_{11}$ hold true as β changes.
- $B_{12} + C_{22} + B_{11} + C_{21} = A_{12} + D_{22} + A_{11} + D_{21}$ and $A_{22} + D_{12} + A_{21} + D_{11} = B_{22} + C_{12} + B_{21} + C_{11}$ hold true as γ changes.

A minimization method can be applied to one or more of the equations. For example, the equation $U = V$, defines an energy function $E = (U - V)^2/2$. The goal of centering is to move to the direction where the energy function can be minimized. In order to minimize E , calculate

$$J = \frac{\partial E}{\partial p} = (U - V) \left(\frac{\partial U}{\partial p} - \frac{\partial V}{\partial p} \right)$$

and

$$H = \frac{\partial^2 E}{\partial p^2} \approx \left(\frac{\partial U}{\partial p} - \frac{\partial V}{\partial p} \right) \left(\frac{\partial U}{\partial p} - \frac{\partial V}{\partial p} \right),$$

in which, p is y , z , α , β or γ . Solving $H\Delta p + J = 0$ provides the direction of the offset movement for all the dimensions except x . To calculate x , the energy function

$$E = \frac{1}{2} \sum_{i=1}^2 \sum_{j=1}^2 (A_{ij}^2 + B_{ij}^2 + C_{ij}^2 + D_{ij}^2)$$

can be used, based on the fact that all the readings go to minimum when x approaches zero in the centered position. Once the plates have been centered, this yields

$$\Delta x = -\frac{\partial E}{\partial x} / \frac{\partial^2 E}{\partial x^2},$$

where

$$\frac{\partial E}{\partial x} = \sum_{i=1}^2 \sum_{j=1}^2 \left(A_{ij} \frac{\partial A_{ij}}{\partial x} + B_{ij} \frac{\partial B_{ij}}{\partial x} + C_{ij} \frac{\partial C_{ij}}{\partial x} + D_{ij} \frac{\partial D_{ij}}{\partial x} \right)$$

and

$$\frac{\partial^2 E}{\partial x^2} \approx \sum_{i=1}^2 \sum_{j=1}^2 \left(\left(\frac{\partial A_{ij}}{\partial x} \right)^2 + \left(\frac{\partial B_{ij}}{\partial x} \right)^2 + \left(\frac{\partial C_{ij}}{\partial x} \right)^2 + \left(\frac{\partial D_{ij}}{\partial x} \right)^2 \right).$$

C. Short range & Latching

Once the medium range has brought the plates within range, the third phase remains. In the short range process, the two mating modules are moved together in the correct general direction in an open loop fashion. This relies upon the mechanical features of the module surfaces (discussed above) and compliance of the entire system to guide the modules.

To determine the correct general direction, the inverse kinematics routines used in the long range process are again used. However, instead of aiming for a fixed goal position, it is a sequence of forward, left and right motions with respect to the currently moving docking plate. These motions use only the joint angle sensors, and rely on the physical contact of the plates to guide the motions.

D. Results

Connecting and disconnecting was successfully demonstrated with seven G2 modules in two arms (a six-module arm and a one-module arms) moving in a single plane (reducing the problem to a three degree of freedom workspace). The arm starts some distance away (shown in Figure 7a) and uses the long range method to move to the state in Figure 7b. The two faces of the mating modules are now close enough that the medium range method can take over. Figure 7c shows the result after this second phase. At this point the two latches are opened and the final stage commences, resulting in the modules successfully docking (Figure 7d). Figure 7e shows the release of the latch on the other side of the arm. So a complete reconfiguration has now taken place: the arm has grown by adding the extra module to its end.

1) *Long range*: The long range motion was tested with up to 24 modules moving in a planar workspace. The torque limits in the G2 modules would not support a chain that long in the non-planar case. Using some *ad hoc* biases to compensate for system hysteresis, the 24 module arm is able to consistently bring the plates of its two end modules to within the medium phase region of acquisition.

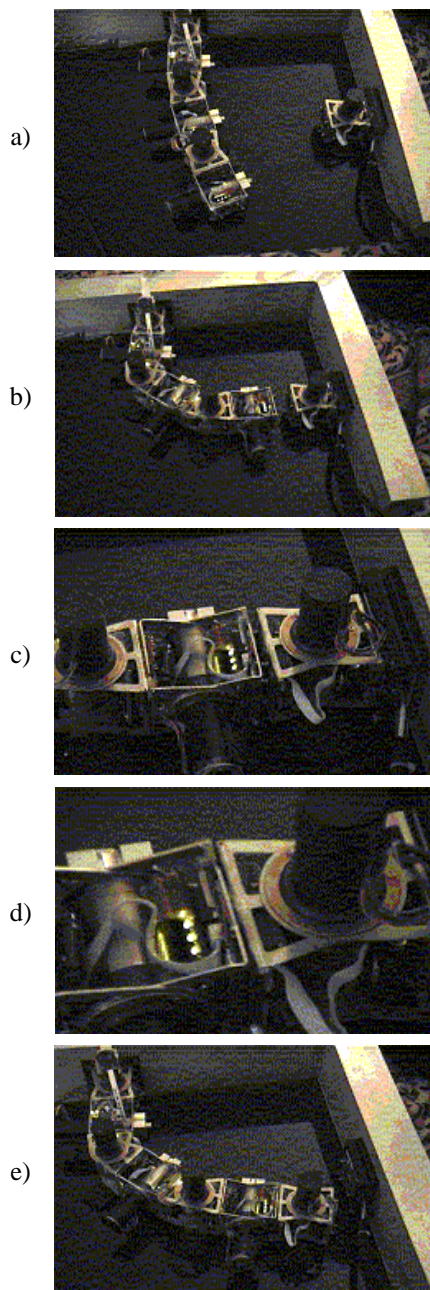


Fig. 7. a) The initial starting position, with the two plates arbitrarily far, b) the end of the long range phase, c) the end of the medium range phase, d) successfully docked, e) end module detached from frame

2) *Medium range:* The computed offset method suffered from inaccuracy and variability of sensor/emitter model, causing the constraint solver to fail. These inconsistencies are formed from irregularities in the mounting of the sensors as well as part-to-part variations.

In addition, the nature of the IR model's curve gave usable sensitivity over only a small range of offsets. The narrow focus lenses on the emitters and receivers made the system highly sensitive to the angle parameters. This high sensitivity existed over a small range of motion, leading to either saturation or no measurable signal over the rest of the range.

A further difficulty proved to be the geometric layout of the sensors and emitters. As both components were recessed

slightly in the frames (for physical robustness), then at close ranges, measured intensity diminished to zero, even when perfectly aligned. This meant that at a distance of about 20mm the sensors became useless.

The problems that lead to the computed offset's failure have been addressed in the new design, as discussed in Section IV.

The centering method proved much more robust to sensor errors and more consistently brought the mating modules to within an acceptable starting position for the short range phase to succeed.

3) *Short range:* Once in phase three, a G2 module opens the latch and inverse kinematics are used to make incremental movements forward (normal to the mating plate planes which are theoretically aligned at this point). After a specified time delay the latches are allowed to close and docking is completed. The success of the short range phase is highly dependent on the medium range phase bringing the mating modules close enough.

It was found that after the latches are allowed to close, it is beneficial to add orthogonal perturbations ("wiggling") to ensure a proper fit. This greatly increased the probability of a successful secure docking. There is precedent for this in other situations, such as industrial assembly tasks.[17]

IV. POLYBOT G3 CONNECTION

A third generation PolyBot module has been prototyped. This new design addresses a number of the shortcomings discovered in G2 and discussed in the previous section.

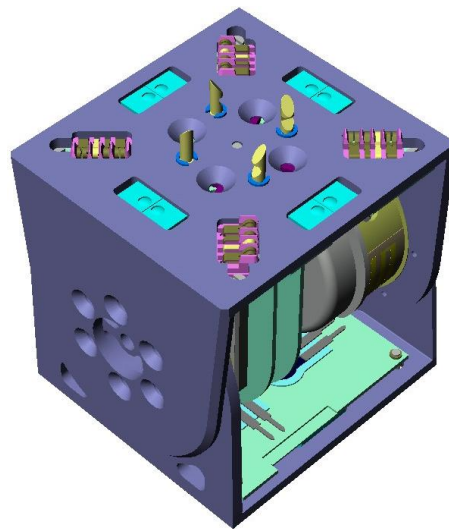


Fig. 8. PolyBot G3 module

The G3 modules are smaller, roughly $50 \times 50 \times 50$ mm. The most notable visible difference is the absence of the DC motor extending past the side of the module. Instead a DC pancake motor with a harmonic gear completely internal to the module is used.

Figures 8 and 9 show the G3 module. The general concept is identical, but the G3 interface plates are slightly smaller than the G2 interface plates, and many of the G3 components have been moved relative to their G2 positions. The changes in the design are made to

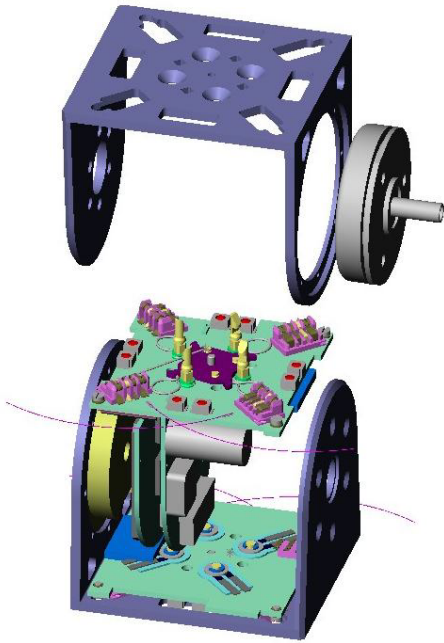


Fig. 9. PolyBot G3 module components

- enhance performance: the connectors are larger pitch and have higher contact force for higher current loads
- add functionality: the pins and latch plate are redesigned so they could be passively latched
- ease assembly: the SMA wires (not shown) are held by the four set screws at the corners and are wound through guide pins on the latch plate—no turnbuckles
- reduce cost: the BeCu spiral spring is replaced with multiple bent wire springs
- better latching: the latch plate is now pinned in the center to both the frame and circuit board so that it rotates consistently about the center
- ease docking: the IR components are moved so that they are now visible to each other during all phases: long range, medium range, short range and even after docking

A. Long range

While the general method for long range positioning using the G3 modules is essentially the same as G2, some changes have been made that can improve the process.

As discussed earlier, the error in the positioning of the end point increases as the number of modules within a chain increases. To the first order, a simple analysis can be made for an simplified case. If a single chain of modules is fixed at one point, and each module contains a small random error in its joint angle, then the error in the position of the chain's other end will be linearly dependent on the number of modules.

As the number of modules increases, the ability for the long range method to bring the endpoint modules within the desired error region may eventually be exceeded. For this case an intermediary stage between the long and medium range process can be inserted. In this stage a spiral search process is used, using the IR sensors to detect when the docking modules come into range to start the medium range process.

Alternatively, *ad hoc* methods may be used to reduce some of the error dimensions. For example, moving both docking modules to contact the ground or another common object will constrain the error space and reduce the dimensionality of the problem.

B. Medium range

The G3 modules have a different arrangement of the IR emitters and detectors. The new design places four emitter-detector pairs on the center of four edges. Figure 10 shows the new mechanical layout of the plate, a filled circle denotes an emitter and an open circle denotes a detector. The new design has the property that when two centered faces are closer, the intensities received from the corresponding emitters are larger. This is in contrast to the G2 design where the intensities diminish (and eventually vanish) due to large emitter-detector angles.

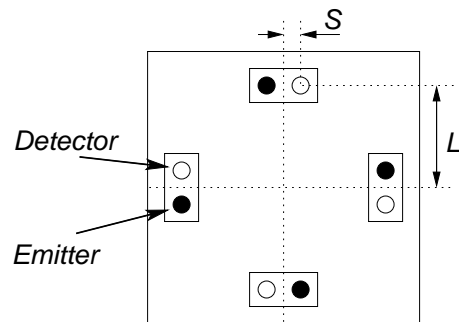


Fig. 10. Mechanical design of the IR 6 DOF sensing device on a PolyBot faceplate

The new design also enables local communication for two connected modules. This allows recognition of which of the two plates are connected and which of the four possible orientations the two connected plates are in. This information is important for automatic configuration recognition during the initialization of a modular self-reconfigurable system. Using IR emitter/receiver pairs in this fashion for modular robots was first shown in [23].

While the G2 arrangement used lensed IR emitters that resulted in model parameters highly dependent on the incident angles, the G3 diodes chosen have no lenses, and a more Lambertian emission property. Now the dominating parameter is the distance between the emitter and detector and not the angles between them. Since the position of the diodes is much easier to control than the angle they are mounted to, the manufacturing assembly errors are no longer as significant. The intensity versus distance curve is shown in Figure 11, which also shows a close fit with the model.

With an increase in the number of IR detectors, measurements from just one plate's sensors is sufficient. Each emitter on one plate is activated in turn. Each of the four detectors in the opposite plate take a reading each time. These 16 samples (after subtracting ambient light readings) are sufficient to solve for the 6D offset transform using Newton/SVD as discussed in Section III-A. The ambient light level readings are updated frequently to ensure robustness even in rapidly changing light conditions.

The IR emitter and receivers were tuned so that the intensity model would be well conditioned in the 10–50mm range. This

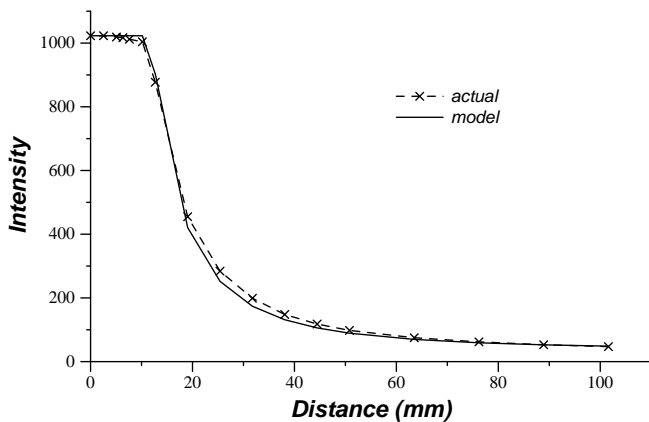


Fig. 11. The actual and model intensity curves for G3

is apparent from the graph in Figure 11. Within this range, the computed offset method (which failed in G2 due to IR model sensitivity) can now be used.

Outside of this range, where the model does not yield useful information, the same centering method of G2 is used. The G3 version of these equations, modified to model the new emitter and detector geometries, prove to be more linear. This increase in linearity, and the reduction in the sensitivity to manufacturing and assembly tolerances should result in corresponding improvements in the centering method as well.

C. Short range and latching

The short range phase is also improved in the G3 system. In G2, the latch hooks are commanded to open before the final phase of docking. SMA actuators are notoriously slow and this process typically takes on the order of ten seconds. In G3 the latch plate can be pushed aside by the pins during insertion without first opening latch. The force required to insert one set of four pins into a frame is measured at just over 1.5kg.

D. Results

While only small numbers of the G3 modules have been produced, and these are going through rapid cycles of minor design modification, some preliminary results exist. Within a single horizontal plane, a chain of seven modules attempts to dock with an eighth (similar to the task shown in Figure 7).

1) *Long range:* From any given starting position, the long range (inverse kinematic) approach correctly maneuvers the two docking faces to a point approximately 30mm apart. For a chain of this length, the strategy could undoubtedly perform much better; the fixed piece of tubing helps by reducing the number of joint errors and interfaces. However as discussed previously, with long chains the inevitable build-up of error in any open loop algorithm makes too close an approach inadvisable.

2) *Medium range:* The medium range strategy (using the computed offset method) has been shown to work experimentally until about 10mm. This is in accordance with Figure 11, which shows 10mm to be around where the IR receivers are near saturation. At this saturation point, the IR model used breaks down. This leaves the pins of each face just about level with

(though possibly slightly mis-aligned with) the holes of the mating module.

Moving onto the centering method, the medium range strategy steers the faces to within about 1mm of perfectly docked.

3) *Short range and latching:* Now the pins are correctly aligned with, and most of the way into, the opposite holes. The final step of docking has not been entirely successful due to very demanding tolerances in the latch mechanisms. The frames are in the process of being modified to resolve this issue, and complete autonomous docking is anticipated soon.

V. CONCLUSIONS

This paper presents some of the issues involved in the docking of chain type self-reconfigurable robots. It describes a three phase approach to docking which should be general for all chain type self-reconfiguration. Several methods are proposed for the medium range phase, where the closed-loop control resides. In experimental verification, a centering control method is empirically found to be more robust than a computed offset method. A third generation PolyBot module system is being tested in which the guidance system for the medium range phase is better suited to both centering and computed offset methods. Experiments to date have tentatively confirmed that this results in more robust and reliable docking.

Acknowledgments

This work is funded in part by the Defense Advanced Research Project Agency (DARPA) contract # MDA972-98-C-0009.

REFERENCES

- [1] M. Yim, D. Duff, and K. Roufas, "PolyBot: a modular reconfigurable robot," in *International Conference on Robotics and Automation*, San Francisco, California, USA, Apr. 2000, IEEE, pp. 514–520.
- [2] S. Murata, H. Kurokawa, and S. Kokaji, "Self-assembling machine," in *International Conference on Robotics and Automation*, San Diego, California, USA, May 1994, IEEE, pp. 441–448.
- [3] C. J. J. Paredis and P. K. Khosla, "Synthesis methodology for task based reconfiguration of modular manipulator systems," in *International Symposium on Robotics Research*, Hidden Valley, PA, USA, Oct. 1993, IEEE, pp. 2–5.
- [4] D. Tesar and M. Butler, "A generalized modular architecture for robotic structures," *Manufacturing Review*, vol. 2, no. 2, pp. 91–118, June 1989.
- [5] M. Yim, D. Goldberg, and A. Casal, "Connectivity planning for closed-chain reconfiguration," in *Sensor Fusion and Decentralized Control in Robotics Systems III*, Boston, MA, USA, Nov. 2000, SPIE, pp. 402–412.
- [6] T. Fukuda and S. Nakagawa, "Dynamically reconfigurable robotic system," in *International Conference on Robotics and Automation*, Philadelphia, USA, Apr. 1988, IEEE, pp. 1581–1586.
- [7] S. Hirose, "Super mechano-system: new perspective for versatile robotic system," in *7th International Symposium on Experimental Robotics*, Honolulu, Hawaii, USA, Dec. 2000, pp. 249–258.
- [8] H. B. Brown, Mvande Weghe, C. Bererton, and P. K. Khosla, "Millibot trains for enhanced mobility," Submitted to *IEEE Transactions on Mechatronics*.
- [9] D. Rus and M. Vona, "Crystalline robots: self-reconfiguration with compressible unit modules," *Journal of Autonomous Robots*, vol. 10, no. 1, pp. 107–124, Jan. 2001.
- [10] K. Kotay, D. Rus, and M. Vona, "Using modular self-reconfiguring robots for locomotion," in *7th International Symposium on Experimental Robotics*, Honolulu, Hawaii, USA, Dec. 2000, pp. 259–269.
- [11] J. W. Suh, S. B. Homans, and M. Yim, "Telecubes: mechanical design of a module for a self-reconfigurable robotics," in *International Conference on Robotics and Automation*, Washington, DC, USA, May 2002, IEEE, pp. 4095–4101.

- [12] C. Ünsal, Kiliççöte, and P. K. Khosla, “A modular self-reconfigurable bipartite robotic system: implementation and motion planning,” *Journal of Autonomous Robots*, vol. 10, no. 1, pp. 23–40, Jan. 2001.
- [13] K. Hosokawa, T. Tsujimori, T. Fujii, H. Kaetsu, H. Asama, Y. Koruda, and I. Endo, “Self-organizing collective robots with morphogenesis in a vertical plane,” in *International Conference on Robotics and Automation*, Philadelphia, USA, Apr. 1988, IEEE, pp. 2858–2863.
- [14] E. Yoshida, S. Kokaji, S. Murata, K. Tomita, and H. Kurokawa, “Micro self-reconfigurable robotic system using shapememory alloy,” in *Distributed Autonomous Robotic Systems*, Knoxville, Tx, USA, 2000, pp. 145–154.
- [15] A. Pamecha, C. Chiang, D. Stein, and G. Chirikjian, “Design and implementation of metamorphic robots,” in *Design Engineering Technical Conference—Computers and Engineering*, Irvine, CA, USA, Aug. 1996, ASME, pp. 1–10.
- [16] M. Yim, “New locomotion gaits,” in *International Conference on Robotics and Automation*, San Diego, California, USA, May 1994, IEEE, pp. 2508–2514.
- [17] W. M. Shen and P. Will, “Docking in self-reconfigurable robots,” in *International Conference on Intelligent Robots Systems*, Maui, Hawaii, USA, Nov. 2001, IEEE/RSJ.
- [18] S. Murata, H. Kurokawa, E. Yoshida, K. Tomata, and S. Kokaji, “A 3-D self-reconfigurable structure,” in *International Conference on Robotics and Automation*, Leuven, Belgium, May 1998, IEEE, pp. 432–439.
- [19] M. Badescu and C. Mavroidis, “Novel smart connector for modular robotics,” in *International Conference on Advanced Intelligent Mechatronics*, Como, Italy, July 2001, IEEE/ASME, pp. 880–887.
- [20] M. Nilsson, “Heavy duty connectors for self-reconfigurable robots,” in *International Conference on Robotics and Automation*, Washington, DC, USA, May 2002, IEEE, pp. 4071–4076.
- [21] A. Casal, *Reconfiguration planning for modular self-reconfigurable robots*, Ph.D. thesis, Stanford University, 2002.
- [22] A. Castano, W.M. Shen, and P. Will, “CONRO: Towards deployable robots with inter-robot metamorphic capabilities,” *Journal of Autonomous Robots*, vol. 8, no. 3, pp. 309–324, July 2000.
- [23] M. Yim, *Locomotion with a unit-modular reconfigurable robot*, Ph.D. thesis, Stanford University, 1995.